

EARLY SEPSIS DETECTION FROM ICU DATA USING WAVELET FEATURE EXTRACTION WITH HYBRID DEEP LEARNING FRAMEWORK

Dr. V. GOKULA KRISHNAN^{1,*}, Dr. PINAGADI VENKATESWARA RAO², Dr. K. SREERAMAMURTHY³, Dr. R. DHARMAPRAKASH⁴, Dr. B. PRATHUSHA LAXMI⁵

^{1,*}Professor, Department of CSE, Easwari Engineering College, Ramapuram, Chennai, Tamil Nadu, India

²Associate Professor, Department of CSE, CVR College of Engineering, Hyderabad, Telangana, India

³Professor, Department of CSE, Koneru Lakshmaiah Education Foundation, Hyderabad, Telangana, India

⁴Professor, Department of EEE, Panimalar Engineering College, Chennai, Tamil Nadu, India

⁵Professor and Head, Department of AI & DS, R.M.K College of Engineering and Technology, Gummidipoondi, Tamil Nadu, India

Email: ^{1,*}gokul_kris143@yahoo.com, ²drrao.pinagadi@cvr.ac.in, ³sreeram1203@gmail.com, ⁴rdharmaprakash@yahoo.co.in, ⁵hod_ads@rmkcet.ac.in

ABSTRACT

For patients in intensive care units (ICUs) to have better outcomes after suffering from sepsis, a potentially fatal illness, prompt and precise identification is essential. Timely care and better patient outcomes depend on early sepsis detection. It is common for traditional diagnostic procedures to miss the early signs of sepsis, which means that treatment is delayed. Using the open-source MIMIC-III clinical database, we provide a new hybrid diagnostic system for early sepsis identification that makes use of deep learning, signal processing, and metaheuristic optimisation. We start by using physiological time-series data including temperature, respiration rate, blood pressure, and heart rate to extract robust, multi-scale, and noise-resistant features using the Wavelet Scattering Transform (WST). Afterwards, a one-dimensional input-adapted AlexNet-based Convolutional Neural Network is trained with these features to learn the high-level feature representations necessary to differentiate among septic and non-septic patients. We optimise hyper parameters including learning rate, filter sizes, and dropout rates using the Hunger Games Search (HGS) method, a new metaheuristic inspired by nature, to further enhance model accuracy and generalisation. Benchmark CNN architectures and traditional machine learning models are outperformed by the suggested WST-AlexNet-HGS pipeline. Classification performance above 95% as shown by evaluation measures like accuracy, precision, recall, and F1-score, demonstrating strong diagnostic reliability. Given the model's efficacy, it might be used as a clinical decision support tool in intensive care units operating in real-time. This hybrid pipeline demonstrates >95% accuracy in early detection of sepsis from ICU data, outperforming conventional methods. The model's robustness and reliability position it as a viable decision support system for real-time clinical use.

Keywords: *Intensive care units, Hunger Games Search, Wavelet Scattering Transform, Sepsis detection, Convolutional Neural Network, AlexNet.*

1. INTRODUCTION

Worldwide, sepsis is a major health concern because of the danger it poses to people's lives. It impacted 49 million individuals in 2017 and was associated with 11 million avoidable deaths worldwide [1]. The patient's vital signs fluctuate as a consequence of sepsis, an immediate response to an infection—typically a bacterial one. The body's cell count, heart rate, and breathing

patterns can all vary, and these changes have the potential to cause organ failure and death [2]. There are three main phases to the development of sepsis, and the risks and severity of each phase differ. Sepsis is the initial stage of an infection and is marked by a mild reaction with a low risk of death. Severe sepsis is the subsequent stage, and it is characterised by a dramatic deterioration of the elevated chance of death [3]. In the last and most dangerous stage of sepsis, known as septic shock,

the body's reaction to the infection becomes too much, causing many problems and the collapse of multiple organs [4].

The best way to treat and manage individuals with sepsis depends on correctly identifying the various stages of the condition. Serious consequences, including death, can result from delaying treatment [5]. The best way to detect sepsis early and treat it effectively is to raise awareness about its symptoms among healthcare professionals and the general population [6]. There has to be more infections found that intra-abdominal and respiratory infections greatly increase the risk of clinical progression of sepsis [7]. Critically important is the prompt diagnosis of people at risk of sepsis. The severity of the illness, mortality rates, and risk of sepsis can all worsen with a delayed diagnosis [8]. Preventing these effects and improving the patient's prognosis can be achieved by early interventions. Always be on the lookout for signs of sepsis. It is critical to recognise the signs early on in order to take the required steps and stop the disease from getting worse [9]. The fact that severe sepsis is identified in almost 750,000 hospitalised individuals in the US every year is concerning [10]. This issue is significant due to the lack of reliable tools for early-stage sepsis detection. Delayed interventions contribute to over 11 million preventable deaths annually, as per WHO estimates, emphasizing the urgent need for data-driven diagnostic frameworks. Despite technological advancements, current ICU alert systems often fail to recognize subtle sepsis patterns. As sepsis progression is rapid and treatment time-sensitive, it becomes imperative to explore robust AI models capable of acting on physiological data alone.

Fewer deaths occur as a result of prompt diagnosis besides treatment. Detecting sepsis early and accurately remains a difficult clinical issue [11]. There are currently just a small number of electronic technologies for sepsis patient monitoring that can anticipate and identify early warning signals of consequences such multi-organ failure [12]. Nevertheless, a machine-learning algorithm (MLA) is one method that has been created to tackle this problem. This method makes use of ML, which enables computers to learn from data automatically, without the need for explicit programming [13]. ML is a useful tool for problems connected to pattern recognition and data analytics since it can find patterns huge quantities of data. It was Arthur Samuel in 1959 who first proposed this idea.

One common application of data mining in medicine is the categorisation of illnesses according to their links to certain health outcomes [14]. Machine learning is a well-known method for improving forecasting capabilities through the instruction of computers to learn from data. By combining statistical and efficient computational methodologies, this technology has revolutionised data analysis. A couple of primary computer kinds both supervised and unsupervised learning systems have substantially enhanced decision-making [15]. Data analytics makes use of a plethora of data mining methods, including decision trees, sequential patterns, classification, clustering, prediction, and association. In machine learning, a classification strategy is used to make predictions about output using a collection of pre-defined classes or groups. One example is the medical field, where a patient's medical history serves as the training set and the likelihood of a disease diagnosis serves as the predicting attribute [16]. Machine learning's capacity to save time in patient care by detecting illnesses quickly with less patient involvement has attracted a lot of attention in medical industry.

A randomised clinical experiment showed that a machine learning system could predict sepsis, shorten the hospital stay from 13 to 10.3 days, and cut death by 12.4%. The results were astounding. Machine learning algorithms were useful in a recent study that aimed to predict sepsis in intensive care unit patients. Analysing clinical laboratory results and vital signs in adult ICU patients, the algorithms discovered new sepsis predictors [17]. Better results, including lower death rates and shorter hospital stays, were the result of this. The results indicate that the healthcare sector stands to gain a great deal from implementing machine learning strategies, which could lead to better treatment for patients.

The capacity to analyse massive amounts of physiological data in real time and enable rapid clinical decision-making has propelled AI-driven solutions to these limits into the spotlight. Here, the MIMIC-III database is a great resource for building sepsis diagnostic prediction models; it is an extensive set of de-identified health records from intensive care unit patients. Here, we introduce a hybrid AI system for better sepsis detection that integrates deep learning, enhanced signal processing, and optimisation based on biological principles. We use the Wavelet Scattering Transform (WST) to isolate robust and discriminative characteristics from unprocessed physiological time-series data. After that, a

Convolutional Neural Network (CNN) based on AlexNet that has been trained to handle one-dimensional input data is employed. We use the Hunger Games Search (HGS) algorithm, a new optimisation technique inspired by nature, to optimise the deep learning model and prevent it from being configured in an inefficient way. This algorithm helps to fine-tune important hyper parameters including learning rate, filter size, and dropout rate. The main goal of this study is to use the MIMIC-III database of intensive care unit patients to create a reliable diagnostic model for early sepsis diagnosis. Some of the specific objectives are:

- In order to use the Wavelet Scattering Transform to derive useful and noise-resistant characteristics from physiological time-series data.
- In order to effectively classify sepsis, it is necessary to create and train a CNN architecture that is based on AlexNet and can learn hierarchical features.
- To improve diagnostic performance by optimizing the CNN's hyper parameters with the Hunger Games Search algorithm.
- Using common presentation criteria, assess the accuracy and reliability of the suggested model and compare it to conventional learning methods.

Hypothesis: A hybrid diagnostic framework combining wavelet-based feature extraction with deep learning and metaheuristic optimization will significantly outperform traditional models in early sepsis detection accuracy, timeliness, and reliability.

While machine learning has shown promise in sepsis detection, existing models often lack robustness to noisy ICU data and are not optimized for real-time prediction. A proactive, hybrid diagnostic system is crucial to close this gap.

This work focuses on early detection of sepsis using ECG-based physiological signals. It does not incorporate clinical notes, medications, or radiology data. Interpretability and transferability to other datasets remain outside the current scope.

This study adopts an experimental research design involving data preprocessing, feature extraction using WST, classification using AlexNet-based CNN, and hyperparameter optimization using HGS. The evaluation is carried out using cross-validation and standard classification metrics.

The rest of the paper is organized as follows: Section 2 mentions the related works; Section 3 provides the proposed methodology in detail; Section 4 discusses the result analysis and finally, the conclusion is made at Section 5.

2. RELATED WORKS

A method called ML-SVM, which is based on machine learning, has been proposed by Abd El-Aziz & Rayan [18] to deal with the issue. Examining intensive care unit monitoring records for subtle changes and early warning signals in order to provide a dependable forecast of sepsis onset is the objective. By assisting healthcare professionals in making informed decisions in a timely manner, this technology-driven method supplements their clinical judgement. The ML-SVM algorithm provides an accuracy of 95.2% when it comes to automating the prediction of sepsis start, with a sensitivity of 91% and a specificity of 93%. This high-Overall Performance version improves upon current methods, allowing medical professionals to make better decisions more quickly and reducing the likelihood of complications associated with sepsis. Reduced affected person impacts, saved lives, decreased healthcare costs, and lessened stress on healthcare specialists in critical care situations are all possible thanks to the ML-SVM technique's optimisation of resource allocation and improvement of early detection.

In order to facilitate early detection besides treatment of sepsis, Shi et al. [19] created a prediction model based on machine learning that utilises clinical data composed within the first twenty-four hours of intensive care unit admission. The electronic medical records of patients with sepsis were analysed using machine learning approaches in this retrospective cohort study that involved many centers. We compared healthcare systems in the United States and China to see how well our models predicted sepsis outcomes within the first twenty-four hours of intensive care unit admission. When compared to more conventional methods, machine learning models for sepsis outcomes using 31 clinical characteristics performed far better. During testing, machine learning approaches produced scores of 0.78 and AUCs above 0.8, in contrast to linear regression's low scores of 0.25. Importantly, when subjected to external validation, these models continued to exhibit strong performance (scoring 0.63-0.77). By aiding clinical decision-making and allowing for early identification and prompt management in the crucial first twenty-four hours after intensive care

unit admission, sepsis prediction models based on machine learning have the potential to greatly improve patient outcomes.

The unique machine learning models presented by Lin et al., [20] make use of full blood count with differential (CBC+DIFF) data, which is a standard, non-invasive test for identifying sepsis because it measures the measurements. Implementing this model within an AI-CDSS to improve critical care sepsis identification and management was the main target. From September to December 2023, researchers at Tri-Service General Hospital looked back at data from 746 intensive care unit patients who were thought to have pneumonia-induced sepsis, as confirmed by radiographs and a SOFA score increase of two points or more. They compared these patients to 746 healthy outpatients who served as controls. Results from Film Array, blood cultures, or positive sputum cultures verified the sources of sepsis infections. Data from September to November was utilised for training purposes, whereas data from December was utilised for validation. The dataset included both fundamental hematological parameters and advanced neutrophil features, such as side scatter light intensity, cytoplasmic complexity, and neutrophil-to-lymphocyte ratio. A number of machine learning models were trained using CBC+DIFF data and evaluated using AUC, sensitivity, and specificity. These models included a gradient boosting classifier, a random forest classifier, and a light gradient boosting machine (LGBM). With the help of workshops and training sessions, the AI-CDSS was able to include the top-performing model. Out of 1492 total cases, 654 (43.8%) were found to be sepsis, as determined by pathogen identification in intensive care unit patients; this included 243 Film Array-positive, 411 culture-positive, and 92 undiscovered cases. Predictive accuracy was good across the board for the ML models; LGBM had the best area under the curve at 0.90, followed by the random forest classifier at 0.89, and the gradient boosting classifier at 0.88. We constructed our AI-CDSS on top of the best-performing LGBM model. It is web-based and allows for quick sepsis risk assessment with CBC+DIFF data.

Examining the possibility of several diagnostic and prognostic sepsis biomarkers as indicators for sepsis and septic shock was the goal of Sater et al., [21]. Methods: In all, 47 patients afflicted with sepsis participated in the research, 11 of them had septic shock. The evaluation included seventeen biochemical, hemostatic, and inflammatory indicators, in addition to blood and

Deep Throat Aspiration (DTA) cultures. To detect biomarker levels in the blood, ELISA was employed. The results showed that septic shock was substantially linked with plasma bilirubin and platelet count (PLT). In 9.1% of septic shock samples and 11.1% of sepsis samples, respectively, no growth was seen ($P = 0.10$). In septic shock patients, there was a statistically significant decrease in *Acinetobacter* (0% vs. 38.9%, $P = 0.02$) and an increase in *Candida* (45.5% vs. 13.9%, $P = 0.039$). Pathogen cultures indicated a preponderance of *Candida* and a dearth of *Acinetobacter*, lending credence to the study's conclusion that PLT and plasma bilirubin may serve as indicators of septic shock.

In order to forecast the likelihood of ICU for patients with SA-AKI, Chen et al., [22] trained machine learning models on the MIMIC-IV database. The electronic research database is used for external validation. We used input to restrict the selection of critical features, including as lab results, vital signs, and comorbidities, down to 24 predictive factors for 9,474 SA-AKI patients in MIMIC-IV. We used Grid Search to optimise the hyper parameters of an Extreme Gradient Boosting (XGBoost) model that we constructed to predict in-hospital mortality. SHapley Additive Explanations (SHAP) improved the model's interpretability. The eICU database was used for external validation. With a 95% confidence interval of 0.859 to 0.897, the suggested XGBoost model was able to obtain an AUROC of 0.878. Among the most important factors that SHAP found to be predictive of death were respiratory rate, serum lactate, and Sequential Organ Failure Assessment (SOFA). Blood lactate, total urine output, serum calcium, and the Acute Physiology and Chronic score were emphasized as important aspects by LIME.

When compared to PCT and C-reactive protein, Roccaforte et al., [23] assessed the predictive efficacy of cell population data (CPD) early identification of sepsis in the intensive care unit (ICU). Additionally, the impact of renal purpose on CPD, PCT, and CRP was examined in both septic and non-septic individuals. Patients self-confessed to the intensive care unit (ICU) at Milan's Edoardo Bassini Hospital in a sequential fashion were the subjects of this retrospective, observational, single-center study. Using the Sepsis-III criteria, patients were categorized as either septic or non-septic. There was no sepsis in the critically sick individuals who made up the control group. Sepsis patients and those with septic shock were further subdivided. Parameters for PCT and CRP, as well as neutrophils' complexity (NE-

SSC), fluorescence intensity (NE-SFL), and width of dispersion were significantly different patients. Using PCT, NE-FSC, NE-WY, NE-WZ, and MO-X, we were able to distinguish between individuals with sepsis and those with septic shock. Renal function did not affect CPD values. When it came to predicting sepsis, CPD, PCT, and CRP all demonstrated different levels of diagnostic presentation efficiency. In terms of overall diagnostic performance for sepsis, the best instruments were NE-SFL, NE-WX, MO-X, MO-Y, PCT, and CRP. Results from this research point to the possibility that NE-SFL besides MO-X, two CPD measures, can aid in the detection and treatment of sepsis.

3. PROPOSED MODEL

In this section, the detection process is carried out by advanced deep learning model and it is visually shown in Figure 1, where each block is described in the upcoming section.

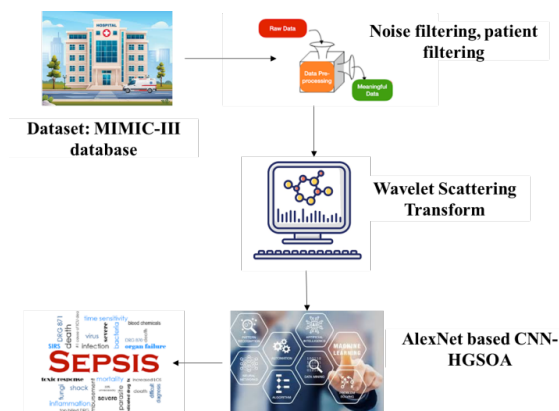


Figure 1: Workflow of the Research Model

3.1. Data Description

All of the electronic health records (EHRs) of critical care database [24]. Patient demographics, medical history, treatment plans, prescriptions, lab results, vital signs, and other clinical data are all part of the database. You can find it on PhysioNet, and anyone can see it [25]. In addition to the MIMIC-III clinical database, which contains a number of physiological signals including ECG, ABP, PPG, and respiration, there is also the MIMIC-III Waveform Database Matched Subset. Both the MIMIC-III clinical database and the bedside monitors have been continuously

recording it in real-time. By matching the waveform records to the MIMIC-III clinical database, the associated clinical records of 10,282 intensive care unit patients are also made available.

3.2. Sepsis Label Definition

When diagnosing sepsis, there are standardized clinical scores that can be used to evaluate the harshness of the condition: SIRS, NEWS, or MEWS. Nevertheless, these scores should not be used for ongoing risk assessment of sepsis. The latest revisions to definition besides diagnostic criteria for sepsis, known as Sepsis-3 criteria, were announced not long ago [26]. Additional information about when sepsis begins can be found in the criteria, which include the time of infection suspicion Failure Score. In order to determine the suspicion of infection time, we use the SI criteria proposed in [27]. The third set of criteria for sepsis suggests that the suspicion of infection window should be defined as the time when SOFA score rises by two points or more. We define sepsis onset time by slightly revising the clinical database queries hourly.

3.3. Dataset Preprocessing

Specifically, this effort is accommodating the waveform database in addition to the clinical database. Specialized tasks, such as annotation and training, are carried out by each database. Applying Sepsis-3 criteria, the clinical database is used to ascertain the timing of sepsis onset. A subsequent step involves annotating the available ECG recordings using the computed onset time. Demographic information, the time of sepsis onset, and the timing of intensive care unit admission and discharge are the primary uses of the clinical database. The prediction model does not take into consideration features like vital signs, lab measurements, or comments from nurses or doctors. Only an annotated waveform database is used to train the predictive model. The three-stage preprocessing method is dependent on availability and quality of ECG recordings.

1) Patient Filtering

We refine our cohort in our settings in the following way. All patients must be at least 15 years old before they can be considered. We also do not include patients whose intensive care unit admission or discharge records are lacking.

Because lab values are necessary for calculating the suspicion of infection time, we also drop patients from the CareVue system when they do not have enough of them. The time of sepsis onset is determined after data filtering. Every patient in the clinical database is also given the International Classification of Diseases, 9th Revision, which is a system of codes used to record medical diagnoses and procedures related to hospitalization. Lastly, before admitting the control patients to the intensive care unit, we double-check their ICD-9 codes to make sure they do not have sepsis. There are a total of 17,725 individuals with sepsis and 17,790 healthy controls in the clinical database. With this query configuration, we can label the waveform database and determine which patients are parts of the study.

When we analyse the waveform database, we run across a lot of problems. There are 10,282 unique intensive care unit patients in the dataset, and a header file is included with every recording. You can't play the recordings without the header files. On the other hand, 187 patients are missing a header file. You can find ECG recordings that are anywhere from a few hours to a few days long. The waveform database only contains the waveforms of 447 sepsis patients because it is a subset of database. An illustration of the sudden shift in signal strength, as seen in Figure 2, reveals a period of relatively low variance.

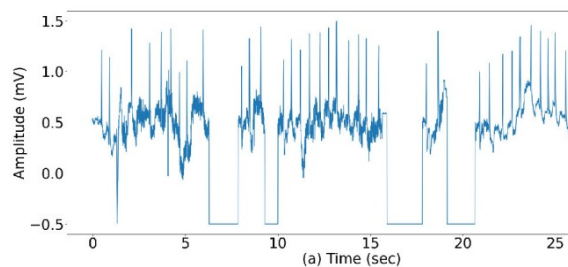


Figure 2: 30 trial recording illustrates abrupt signal alteration for Subject ID= 69339

Furthermore, 53,319 patients were included in the analysis that did not develop sepsis. It is not uncommon for a single patient's record to contain numerous waveform record pairs. A significant time gap separates these record pairings, which poses a problem even if they are associated with the same intensive care unit stay. Since there may be more than one recording for a given intensive care unit stay, we will only take into account the first recording or those recorded closest to the period when sepsis first appeared. While

each patient's ECG waveform is stored in the database, the available ECG leads display discrepancies. Patients whose ECG waveforms were recorded by lead II are thus the only ones included in our cohort. In addition, we only take into account a single hospitalization for patients who have been to the intensive care unit multiple times. Also, we check the record beginning and ending times against the ICU in-time and out-time. It was found that there is a discrepancy due to multiple admissions to the intensive care unit, even if subject id is noticed in both databases. As an example, subject 188 was admitted to the MICU and SICU eight times. The patient's entrance time was reported as "2161-07-01 19:44:00," yet the waveform database does not have information for this stay, even though the patient had sepsis at that period. The admittance time associated with the accessible electrocardiogram record is "2161-12-09-17-50."

Our prediction algorithm zeroes in on the likelihood of sepsis occurring within the next six hours to zero hours at the hourly intervals throughout an intensive care unit stay. For every hour of control, we labeled it 0. If included 12 hours after sepsis begins, there is a better likelihood of discovering its major features. Our data collection for early prediction cases includes instances recorded up to 12 hours after the start of sepsis. The prediction windows are represented by t_{pred} , and labels are set to 1 if t is more than or equal to $t_{onset} - t_{pred}$ and to 0 if t is less than or equal to $t_{onset} - t_{pred}$. In addition, we exclude individuals who develop sepsis before 6 hours. We take up to 48 hours of data from the start of the control patients so that they can have an intensive care unit stay that is comparable in maximum duration. In the clinical sample, the total prevalence of sepsis is around 10%. In our cohort study, we choose the 1:10 ratio to keep the prediction problem reasonable. Table 1 provides a concise overview of the final population data.

Table 1: Demographic statistic of the final cohort

Patient Demographics	Sepsis Group	Control Group
Sum of patients	65	610
Female	33	288
Male	32	322
Age (μ)	79.62	76.25
Entire sepsis hours	17.4h	-
Total ICU length of stay	193.6	84.8h
Ethnicity	Sepsis Group	Control

		Group
White	43	413
Black or African-American	5	63
Hispanic or Latino	1	26
Unknown	10	62
Admission Category	Sepsis Group	Control Group
Elective	7	112
Emergency	58	493
Urgent	-	5
Additional	6	46

2) Filtering Non-ECG Segments

There has been a plethora of research on noise detection and ECG signal quality evaluation. Noise in electrocardiogram (ECG) signals can cause false alarms and incorrect diagnoses, hence it is crucial to be able to identify low-quality ECG signals, especially in a very chaotic setting like an intensive care unit (ICU) [28]. Several problems, such as an abrupt loss of signal, a large number of missing values, poor electrode contact, besides others, might compromise ECG recordings, which we point out. In order to separate the ECG segments from the severely distorted and noisy ones, we employ a pipeline.

- First, we split every recording into two-minute parts. Furthermore, segments that have more than 400 ms of consecutive zero values are also deleted.
- Some segments in the ECG waveform also abruptly vanish. Lastly, if any missing values (represented by NaN) are found in the target segment, we remove that segment.
- The 2-minute segments in question have a low variation; thereafter, it becomes apparent that the waveform database contains a multitude of inverted ECG signals.
- As a result, we are able to identify them and fix the polarity of reversed ECG signals.

Some recordings still display non-ECG waveforms after everything is taken into account. A manual inspection is conducted for these records. We check the non-ECG segment filtering every hour so we can keep track of the stages in time. We fill the corresponding time step with missing data to impute in the subsequent steps if we need to

eliminate all the 2-minute segments in the 1-hour window.

3.4. Feature extraction using Wavelet Scattering Transform

Signal representations generated by a wavelet scattering transform are stable, informative, and translation invariant. Classification is one area where it really shines because of its resistance to deformations and preservation of category discrimination abilities. Its outstanding performance in classification is the reason we can relate to it. Here, we can see the signal being considered as $f(t)$. It is the intention of both the low-pass filter and the wavelet function to generate filters that cover the full frequency spectrum of the input signal. At a specific scale, $\phi(t)$ represents the low-pass filter that produces translation-invariant interpretations of (f) . T . The set of wavelet indices that can resolve frequencies up to an octave Q_k is denoted by Λ_k . By stretching wavelet ψ_j filter banks (ψ_j) can be created. (Convolution $S_0 f(t) = f * \phi(t)$ generates a translation invariant feature of (f) at the local level, even if it results in low-frequency data. These lost high frequencies can be recovered using a wavelet elastic modulus transform.

$$|W_1|f = \{S_0 f(t), |f * \psi_{j1}(t)|\}_{j1 \in \Lambda 1} \quad (1)$$

Averaging coefficients with ϕ_j yields the 2^{rst}- coefficients.

$$S_1 f(t) = \{|f * \psi_{j1}| * \phi_j(t)\}_{j1 \in \Lambda 1} \quad (2)$$

Complement high-frequency coefficient values can be retrieved by taking into account the information that was lost because of averaging. $S_1 f(t)$ as component of $|f * \psi_{j1}|$ as shown in the following equation:

$$|W_2||f * \psi_{j1}| = \{S_1 f(t), ||f * \psi_{j1}| * \psi_{j2}(t)|\}_{j1 \in \Lambda 2} \quad (3)$$

In the second scattering coefficients

$$S_2 f(t) = \{|f * \psi_{j1}| * \psi_{j2} * \phi_j(t)\}_{j1 \in \Lambda i} \quad i = 1, 2, \dots \quad (4)$$

Iterating preceding method harvests wavelet integrand convolutions.

$$U_m f(t) = \{ \{ |f^* \psi_{j_1}|^* \dots |^* \psi_{j_m} \} \}_{j_1 \in \Delta_i}, i = 1, 2, \dots, m \quad (5)$$

Scattering coefficients at m-th order

$$S_m f(t) = \{ \{ |f^* \psi_{j_1}|^* \dots |^* \psi_{j_m}|^* \phi_j(t) \} \}_{j_1 \in \Delta_i}, i = 1, 2, \dots, m \quad (6)$$

The concluding matrix of scattering is

$$S_m f(t) = \{ S_m f(t) \}_{0 \leq m \leq l} \quad (7)$$

Though hard to measure, scattering decomposition could pick up on subtle shifts in the duration and amplitude of electrocardiogram (ECG) signals that do reflect the heart's condition. Therefore, we use a network of wavelet scattering to produce accurate ECG heartbeat representations, which reduces variation within a single arrhythmia class while maintaining sufficient discriminability between them. It is known that the energy of scattering parameters decreases marginally with increasing layer thickness, with nearly all of the energy concentrated in the top two layers. Consequently, we extracted ECG signal properties using a two-request scattering network. The algorithm's complexity is also drastically reduced as a result of this.

3.5. Classification using CNN Model

The original intention of developing the CNN model was to replicate visual processing in humans. The networks' various topologies resulted from the employment of multiple layers organized in various ways. Nonetheless, there are three distinct types of layers that can be identified:

Layers of Convolution: The two-dimensional convolution layers employ trainable filters or kernels to carry out the convolution operations; each kernel can optionally have a trainable bias. When performing convolution, the kernels are "strides" across the input. The general rule is that kernels skip more space between convolutions when stride is larger. Consequently, the output size was reduced and the total number of convolutions was reduced. Each kernel placement

resulted in a multiplication operation kernel, with the bias added to the final product. A feature map with the convolved output was the end product. Typically, an activation function was used to route the feature maps in order to provide input for the subsequent layer. By plugging the input size (N), kernel size (F), padding (P), besides stride (S) into Equation (8), we can get the feature map's output size.

$$Output\ size = \frac{N - F + 2P}{S} + 1 \quad (8)$$

Layers of subsampling: Two-dimensional subsampling layers down-sample input features using non-trainable windows or kernels. In many cases, this reduces the amount of features and makes a network less dependent on location. The two subsample methods that saw the greatest action were average and maximal pooling. There are two ways to calculate the values that should be included in the feature map: the average and the maximum. Just like with convolution layers, the size of the feature map was decided for subsampling layers. Incorporating specific trainable parameters into these layers can help with model learning in general.

Fully Connected Layers: The sole fully connected layers were CNNs. After various convolution and subsampling procedures, they often manifest in the final few layers of the majority of CNNs. An activation function, and multiple hidden layers make up the fully linked layer. Their activities included taking inputs, multiplying them by trainable weight vectors that included a bias, and then adding the results. In the past, the output of these layers was delivered via activation functions, which are similar to convolution layers. In order to prevent over fitting, CNN has discontinued regularization. As a dropout goes through back propagation and forward learning, he or she will randomly assign a value of 0 to many neurons. To prevent the neural network from succumbing to over fitting, this straightforward method is used.

The convolutional neural network (CNN) architecture, including dataset separation and CNN learning, is detailed in this section.

Dataset separation: In order to prepare the dataset for CNN training, it is first divided into two parts: training data besides test data. The information that CNN uses to train itself is called training data. The make-up of the test data and the training data is distinct. After loading the training

data into the software, the 10-fold cross-validation method divides the data into two subsets: the training subset and the validation subset. Once training is complete, the best CNN model will be reloaded and used to make predictions from all test datasets.

CNN learning: The choice of CNN architecture must be made prior to beginning the learning process. An architecture that is well-suited to the dataset will yield the best performance. A CNN based on a tweaked version of the AlexNet architecture was utilised in this research. Both its high performance and its suitability to platforms with restricted capacity, like Android mobile, contributed to its selection as the preferred architecture. One output layer, three completely connected layers, and one convolution layer make up the design. Among the neural network's parameters is the gradient descent method, the most important algorithm for learning (optimizer). Using this algorithm, the weights of every neuron will be adjusted. From adagrad and sgd to adadelta and adam and rmsprop and many more, deep learning is home to a wide variety of optimizers. Using a learning rate of 0.005, the Adam optimizer was employed in this study. One way to determine the adaptive parameter is by using adaptive moment estimation, or Adam. Just like momentum, Adam maintains an exponential decay rate on the prior gradient mt:

$$\hat{m}_t = \frac{m_t}{1-\beta_1^t} \tag{9}$$

$$\hat{v}_t = \frac{v_t}{1-\beta_2^t} \tag{10}$$

Based on the results of equations (9) and (10), we can deduce approximations of the first and second moments, respectively, of each gradient. Afterwards, the parameter's final formula is revised to:

$$\theta_c + 1 = \theta_c - \frac{\eta}{\sqrt{\hat{v}_t + \epsilon}} \hat{m}_t \tag{11}$$

the value of β_1 is 0.9, β_2 is 0.9999, besides ϵ is 10^{-8} .

3.5.1. The Construction of CNN Is based on Alex Net Alteration

This study's CNN is built on the eleven-layer AlexNet construction. Nevertheless, the

writers of this study made fewer layers of modifications. The six-layer AlexNet architecture used in this study connected levels, and a single output layer. The RGB pixels of the input image measure 64×64 . The rectified linear unit (ReLU) initiating operation is used in the 32-filter initial convolution layer with a 3×3 kernel size. Equation (12) demonstrates that ReLU is an activation function.

$$f(x) = \max(0, x) \tag{12}$$

A non-linear transformation is applied to the signal by use of the activation function. Next, a neuron sends its transformed output to the layer below it as an input. By default, it operates with a value of 0, the value equal to the value of x. Following an early Conv2D layer, the 2×2 max pooling layer is applied with ReLU activation function as well, has 64 filters besides a 3×3 kernel size.

Input to the second convolution layer comes from the layer as well as the preceding pooling. In the second maximum pooling layer, the pooling size is 2×2 , and the dropout value is 0.2. The third convolution layer utilises the ReLU are input. The pooling layer is 2×2 , and the dropout value is 0.4. The third convolution layer utilises the ReLU activation function; it has a 3×3 kernel size and a filter size of 128.

All datasets up to flattening layer yield the same amount of according to the AlexNet design. The dense layer will take its input from this flatten layer. The details of CNN using the AlexNet architecture are displayed in Table 2. The activation function utilised in the hidden layer is ReLU. The first hidden layer contains 64 units of neurons, the second 128 units, and the third 256 units. Ten units using a Softmax activation function equal one hidden-layer output, which is equal to the sum of existing classes.

With Softmax, the sum of all components' values is 1, and the results of learning or predictions from earlier layers are distributed over the interval [0, 1]. The CNN-predicted class is the highest-valued output from Softmax. A look at Equation (12) reveals the Softmax function's formula: for every element z, j is the index, and N is sum of elements. Equation (13) is the result of translating the Softmax equation.

$$\sigma(z)_j = \frac{e^{z_j}}{\sum_{k=1}^N e^{z_k}}, j = \{1, 2, \dots, N\} \quad (13)$$

This study's architecture was settled by a series of experiments that focused on the optimal number of layers for a convolutional neural network (CNN) perfect.

3.5.2. Implementation of CNN Based on AlexNet Alteration Construction

Following the completion of the procedure and the set, the CNN Architecture is put into place. Since the design in this study is an adaptation of the current AlexNet made an effort to apply it from the most optimal architecture in this CNN model—four layers—beginning with a single layer.

There is one output, three fully linked layers, and three convolution layers in the efficient AlexNet implementation. Utilizing ReLu functions with dropout levels of 0.2, 0.2, and 0.4 constitutes the layer convolution. At the same time, the output layer employs the dense layer's function.

Compiling the model with the optimizer, loss, and metrics parameters follows model construction. The model compilation process begins with the Adam optimizer being initialized.

The steps per epoch argument, which holds 75 data created to carry out the training model implementation. The argument on the batch size follows. The sum of photos step is 128 and is used as batch size argument. The validity split argument is last one. As a validation approach, a validation split randomly divides the data into two sections. For the validation split, the authors settle on 0.2.

3.5.3. Prediction and Evaluation Using CNN Model

In order to find out how well the top CNN model can extrapolate from its training data, this step is executed. The input for the CNN model came from the test data. The CNN output layer uses function formula to determine the likelihood of each class for each incoming signal. An i-th neuron with greatest predicted output likelihood value is the output of a convolutional neural network (CNN).

Evaluation of representation's efficacy follows. The next step is to compare the model's predictions with the actual data. Each assessment

models -measure scores were calculated using a confusion matrix for convenience.

3.5.3.1. Implementation of CNN Prediction Model

One way to evaluate a training model's efficacy is to put its predictions into action. The predict (•) function is a part of the Keras library that can be used to make predictions about the model. The input signal is prepared to be turned into an array by loading it with a size of 64 × 64. After that, the class of predictions and their corresponding predicted values are computed.

3.5.3.2. Implementation of CNN Evaluation Classical

The accuracy and loss values provided in the model are determined through evaluation of the model. If you want to evaluate your model, you can use the evaluate (•) function in Keras library. The confusion matrix is created during training and shows the model's predictions in terms of recall, accuracy, precision, besides F-measure.

3.5.3.3. Converting Model

Converting the CNN model into a living, breathing organism capable of producing predictions from real-time data is the last stage. After that, Tensor flow Lite is used to transform the CNN model.

By providing developers with the means to execute their devices, Lite paves the way for on-device machine learning. A directory is created with the extension "model" before the conversion begins.

Table 2: AlexNet Construction

Parameters	Layer (Category)	Output Shape
896	Conv2D	(None, 62, 62, 32)
0	MaxPooling2D_2	(None, 6, 6, 128)
0	Dropout 2	(None, 6, 6, 128)
0	MaxPooling2D	(None, 31, 31, 32)
0	Dropout	(None, 31, 32)
18,496	Conv2D_1	(None, 29, 64)
0	MaxPooling2D_1	(None, 14, 64)
0	Dropout_1	(None, 14, 64)
73,856	Conv2D_2	(None, 6, 32)

294,976	Dense	(None, 64)
8320	Dense_1	(None, 128)
8256	Dense_2	(None, 64)
650	Dense_3	(None, 10)

3.6. Fine-tuning using Hunger Games Search Algorithm

The "Hunger Games" search method proposed by Yang [28] for use in the Alex Net model's fine-tuning process takes its cues from the behaviours and actions of animals going through starvation. The majority of HGS animals either cooperate or do not. Shadows are a representation of cooperative behaviour:

$$X(t + 1) = X(t). (1 + randn) \quad (14)$$

where X(t) is the site of current person and randn is the random sum distribution.

The behaviour is unprotected as shadows:

$$X(t + 1) = \begin{cases} W_1 \cdot X_b + R \cdot W_2 \cdot |X_b - X(t)|, & r_2 > E \\ W_1 \cdot X_b - R \cdot W_2 \cdot |X_b - X(t)|, & r_2 < E \end{cases} \quad (15)$$

Where X_b characterises the best exact at the current recurrence, W_1 and W_2 characterise weight of hungry, r_2 R is a range controller, E is a random number among 0 and 1, and the following formulas show the variables that affect the global location:

$$E = sech(|F(i) - BF|) \quad (16)$$

As mentioned earlier, F(i) characterises the fitness entity, BF is best current repetition, formula for sech is as shadows:

$$sech(x) = \frac{2}{e^x + e^{-x}} \quad (17)$$

The limits R, W_1 , and W_2 are exposed as shadows:

$$R = 2 \times shrink \times rand - shrink \quad (18)$$

$$shrink = 2 \times \left(1 - \frac{t}{T}\right) \quad (19)$$

$$W_1(i) = \begin{cases} hungry(i) \cdot \frac{N}{SHungry} \times r_4, & r_3 < l \\ 1, & r_3 > l \end{cases} \quad (20)$$

$$W_2(i) = (1 - exp(-|hungry(i) - SHungry|)) \times r_5 \times 2 \quad (21)$$

here, t represents current restatement, rand is an arbitrary sum between 0 besides 1, besides T is the extreme sum of repeats. We get SHungry, which is the sum of everyone's feelings of hunger, when we multiply the hunger levels of all the swarm members by N. and r_3, r_4, r_5 are unintentional statistics in diversity of [0, 1].

The preparation of $hungry(i)$ is envisioned as underneath:

$$hungry(i) = \begin{cases} 0, & AllFitness(i) == BF \\ hungry(i) + H, & AllFitness(i) \neq BF \end{cases} \quad (22)$$

where iteration keeps their fitness and value of 0. The other values are increased by a value H depending on their prior hunger values. Assisting each individual is a distinct parameter H.

Here is the formula for H:

$$H = \begin{cases} LH \times (1 + r_6), & TH < LH \\ TH, & TH \geq LH \end{cases} \quad (23)$$

$$TH = \frac{F(i) - BF}{WF - BF} \times r_7 \times 2 \times (ub_i - lb_i) \quad (24)$$

where r_6 and r_7 represent a random integer that ranges from 0 to 1, LH is an imperfect limit, F(i) is the fitness penalty for each individual, BF and WF present iteration, and the spaces are where the variables are located.

3.6.1 HGS Pseudo Code

The steps to carry out the HGS operation are detailed in the following pseudo code:

```

1: → Initialize the parameters  $N, T, l_{HGSOA}, D, SHur$ 
2: → Initialize the position of all individuals  $X_i$ 
3: → While( $t \leq T$ )
4: → Calculate the fitness of all individuals
5: → Update  $BF, WF, X_p, BI$ 
6: → Calculate the Hungry using Equation (21);
   Equation (20);
7: → For each individual
8: → Calculate  $E$  using Equation (15); update  $F$ 
   using Equation (14)
9: → End For
10: →  $t = t + 1$ 
11: → End While
12: → Return  $BF$  and  $X_p$ 
    
```

4. RESULTS AND DISCUSSION

The platform that conducted the research had the following hardware specifications: a 16 GB main memory, an 8 GB graphics processing unit (GPU), besides an Intel Core i7 CPU [29]. Ubuntu 20.04 with CUDA9.0, Cudnn7.1, Tensor Flow 1.15, and Python 3.7 were the software specifications, however. The experiments were carried out in at least 16 batches according to these parameters, which allowed the model training procedure to be finished pretty quickly [30].

4.1. Analysis of proposed model on Diverse Training besides Testing Ratio

Figure 3 presents the comparative study of proposed classical on diverse training besides testing ratio that shows the influence of data.

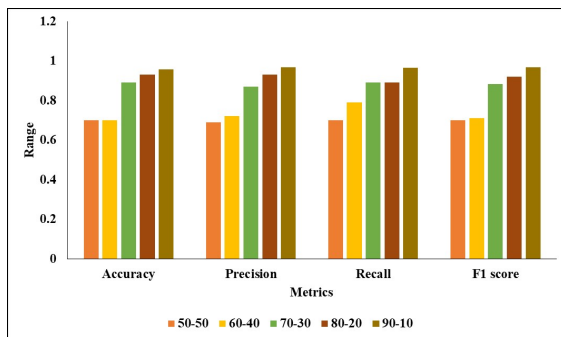


Figure 3: Visual Analysis Of Data Ratio On Proposed Model

The performance of a classification model evaluated under different training-testing splits, ranging from 50-50 to 90-10. As the training data proportion increases, a consistent improvement is observed across all performance metrics score. The 50-50 split yields a modest accuracy of 0.7009 with balanced precision and recall around 0.69–0.70. With a 60-40 split, slight gains are noted, especially in recall (0.79), although the accuracy remains almost the same. A significant boost appears with the 70-30 split, where the accuracy jumps to 0.89 and all metrics show a strong alignment near 0.87–0.89. Further improvement is seen in the 80-20 split, with accuracy reaching 0.93, and both precision and F1 score maintaining high values. The 90-10 split delivers the best overall performance, achieving an accuracy of 0.958, precision of 0.969, recall of 0.964, besides F1 score of 0.967, indicating excellent model generalization when trained on a larger dataset portion.

4.2. Fine-tuning Optimizer analysis

Figure 4 presents comparative investigation of proposed optimizer with existing optimizer for fine-tuning the proposed classifier in terms of diverse metrics.

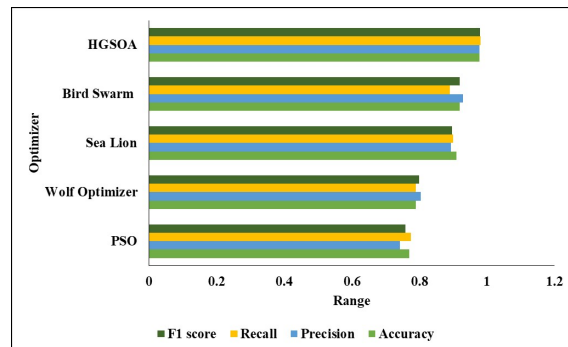


Figure 4: Visual Investigation Of Projected Optimizer With Existing Techniques

The performance of various optimization-based models using score. Among the listed models, HGSOA (Hybrid Gradient-based Swarm Optimization Algorithm) demonstrates the most superior accuracy of 0.978, perfectly balanced precision and recall (0.978 and 0.981), and an impressive F1 score of 0.98, highlighting its strong generalization and robustness. The Bird Swarm model also performs well with a 0.92 accuracy and a high F1 score of 0.92, indicating reliable classification capabilities. The Sea Lion optimizer follows closely with 0.91 accuracy, reflecting a

strong balance between precision and recall. In contrast, Wolf Optimizer and PSO (Particle Swarm Optimization) show relatively lower accuracies of 0.79 and 0.7701, respectively, with moderately aligned precision-recall values. Overall, the HGSOA model outperforms all others in every metric, making it the most effective optimization technique in this comparison for the classification task.

4.3. Classification Analysis

Figure 5 presents graphical study of projected classifier with existing events in terms of diverse metrics.

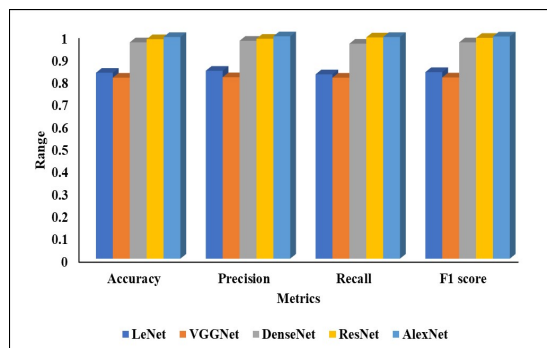


Figure 5: Investigation Of Projected Classifier

The performance metrics of numerous deep learning architectures for a classification task, focusing on score. AlexNet attains highest overall presentation accuracy of 0.991, a precision of 0.994, and a recall of 0.991, resulting in a near-perfect F1 score of 0.993, making it the most effective model in this comparison. ResNet follows closely with 0.981 accuracy and an impressive F1 score of 0.987, reflecting its strong learning capability and deep residual connections that help in minimizing vanishing gradients. Dense Net, known for its dense connectivity, also performs excellently with a 0.967 accuracy and balanced metrics. In contrast, LeNet and VGGNet, being relatively shallower and older architectures, show moderate performance, with LeNet reaching 0.831 accuracy and VGGNet slightly lower at 0.809, indicating their limitations in handling more complex or high-resolution data. Overall, AlexNet and ResNet dominate in score, affirming their suitability for high-accuracy classification applications.

Compared to models such as ML-SVM (accuracy 95.2%) and LGBM (AUC 0.90), our

WST-AlexNet-HGS model achieves higher precision and F1 scores, suggesting improved reliability. These findings are consistent with and extend prior work by integrating robustness to noise through wavelet transforms and parameter tuning via HGS.

5. CONCLUSION

Using patient data from MIMIC-III database, we developed a reliable besides precise framework for automated sepsis diagnosis in this research. In this approach, a hybrid pipeline was used to accomplish the following tasks: multi-resolution feature extraction using Wavelet Scattering Transform (WST); deep feature learning and classification using an AlexNet-based Convolutional Neural Network (CNN) [31]; and hyper parameter optimisation and performance optimisation using a novel metaheuristic algorithm called Hunger Games Search (HGS). Time series physiological signals like temperature, respiration rate, blood pressure, and heart rate were successfully analysed using the Wavelet Scattering Transform, which extracts scale-invariant features with minimal variance. These properties made the signal resistant to frequency and time domain noise and signal distortions that are typical of intensive care unit data. The CNN architecture based on AlexNet, modified for one-dimensional physiological data, allowed for the extraction of abstract representations at a high level, which were critical for early development of sepsis. When compared to learning models, the network's deep layers significantly improved diagnostic capability by accurately modeling hierarchical relationships among clinical features. Hyper parameter optimisation was carried out using Hunger Games Search (HGS) to improve diagnosis accuracy. By emulating the strategy-based decision-making and survival dynamics seen in the fictional "Hunger Games," this algorithm allows for a competitive search mechanism that strikes a balance between exploration and exploitation. HGS greatly improved CNN classification performance by optimizing key parameters as learning rate, number of filters, dropout rate, and kernel sizes.

The proposed WST-AlexNet-HGS pipeline fared better than the status quo in experiments. The scheme's ability to differentiate among septic and non-septic patients was validated through performance evaluation utilizing measures score. These findings prove that the suggested model can be a solid decision-support tool for identifying sepsis in intensive care units at an early

stage. To optimise resource allocation, improve patient outcomes, and reduce mortality, early sepsis diagnosis is crucial. An exciting new path in clinical informatics and IHS is the combination of deep learning, bio-inspired optimisation, and wavelet-based feature extraction. There are a number of avenues that might be investigated to improve the performance and clinical utility of the suggested WST-AlexNet-HGS framework, despite its impressive accuracy in sepsis diagnosis on the MIMIC-III dataset. However, the study does not explore temporal drift in signal characteristics, nor does it assess model interpretability in clinical settings. Future research should investigate these aspects and test the framework in real-world ICU deployments. To better understand the patient's health and provide more accurate diagnoses, future research may concentrate on integrating multi-modal data, including results from laboratory tests, clinical notes, radiological reports, and medication histories.

REFERENCES:

- [1] Gao, J., Lu, Y., Ashrafi, N., Domingo, I., Alaei, K., & Pishgar, M. (2024). Prediction of Sepsis Mortality in ICU patients using machine learning methods. *BMC Medical Informatics and Decision Making*, 24(1), 228.
- [2] Yadgarov, M. Y., Landoni, G., Berikashvili, L. B., Polyakov, P. A., Kadantseva, K. K., Smirnova, A. V., .. & Likhvantsev, V. V. (2024). Early detection of sepsis using machine learning algorithms: a systematic review and network meta-analysis. *Frontiers in Medicine*, 11, 1491358.
- [3] Boussina, A., Shashikumar, S. P., Malhotra, A., Owens, R. L., El-Kareh, R., Longhurst, C. A., ... & Wardi, G. (2024). Impact of a deep learning sepsis prediction model on quality of care and survival. *NPJ digital medicine*, 7(1), 14.
- [4] Kallonen, A., Juutinen, M., Värri, A., Carrault, G., Pladys, P., & Beuchée, A. (2024). Early detection of late-onset neonatal sepsis from noninvasive biosignals using deep learning: A multicenter prospective development and validation study. *International Journal of Medical Informatics*, 184, 105366.
- [5] Ates, H. C., Alshanawani, A., Hagel, S., Cotta, M. O., Roberts, J. A., Dincer, C., & Ates, C. (2024). Unraveling the impact of therapeutic drug monitoring via machine learning for patients with sepsis. *Cell Reports Medicine*, 5(8).
- [6] Pérez-Tome, J. C., Parrón-Carreño, T., Castaño-Fernández, A. B., Nieves-Soriano, B. J., & Castro-Luna, G. (2024). Sepsis mortality prediction with machine learning techniques. *Medicina Intensiva (English Edition)*, 48(10), 584-593.
- [7] Xia, Y., Long, H., Lai, Q., & Zhou, Y. (2024). Machine learning predictive model for septic shock in acute pancreatitis with sepsis. *Journal of Inflammation Research*, 1443-1452.
- [8] Yong, L., & Zhenzhou, L. (2024). Deep learning-based prediction of in-hospital mortality for sepsis. *Scientific Reports*, 14(1), 372.
- [9] Gao, Y., Wang, C., Shen, J., Wang, Z., Liu, Y., & Chai, Y. (2024). Systematic review and network meta-analysis of machine learning algorithms in sepsis prediction. *Expert Systems with Applications*, 245, 122982.
- [10] Shi, J., Han, H., Chen, S., Liu, W., & Li, Y. (2024). Machine learning for prediction of acute kidney injury in patients diagnosed with sepsis in critical care. *Plos one*, 19(4), e0301014.
- [11] O'Reilly, D., McGrath, J., & Martin-Loeches, I. (2024). Optimizing artificial intelligence in sepsis management: Opportunities in the present and looking closely to the future. *Journal of Intensive Medicine*, 4(1), 34-45.
- [12] Bomrah, S., Uddin, M., Upadhyay, U., Komorowski, M., Priya, J., Dhar, E., ... & Syed-Abdul, S. (2024). A scoping review of machine learning for sepsis prediction-feature engineering strategies and model performance: a step towards explainability. *Critical Care*, 28(1), 180.
- [13] Zhang, G., Shao, F., Yuan, W., Wu, J., Qi, X., Gao, J., ... & Wang, T. (2024). Predicting sepsis in-hospital mortality with machine learning: a multi-center study using clinical and inflammatory biomarkers. *European Journal of Medical Research*, 29(1), 156.
- [14] Li, J., Zhu, M., & Yan, L. (2024). Predictive models of sepsis-associated acute kidney injury based on machine learning: a scoping review. *Renal Failure*, 46(2), 2380748.
- [15] Palmowski, L., Nowak, H., Witowski, A., Koos, B., Wolf, A., Weber, M., ... & SepsisDataNet. NRW research group. (2024). Assessing SOFA score trajectories in sepsis using machine learning: A pragmatic approach to improve the accuracy of mortality prediction. *PLoS One*, 19(3), e0300739.

- [16] Yang, S., Guo, J., Xiong, Y., Han, G., Luo, T., Peng, S., ... & Zhang, J. (2024). Unraveling the genetic and molecular landscape of sepsis and acute kidney injury: A comprehensive GWAS and machine learning approach. *International Immunopharmacology*, 137, 112420.
- [17] Agnello, L., Vidali, M., Padoan, A., Lucis, R., Mancini, A., Guerranti, R., ... & Carobene, A. (2024). Machine learning algorithms in sepsis. *Clinica Chimica Acta*, 553, 117738.
- [18] Abd El-Aziz, R. M., & Rayan, A. (2025). Early detection of sepsis using machine learning algorithms. *Alexandria Engineering Journal*, 111, 47-56.
- [19] Shi, S., Zhang, L., Zhang, S., Shi, J., Hong, D., Wu, S., ... & Lin, W. (2025). Developing a rapid screening tool for high-risk ICU patients of sepsis: integrating electronic medical records with machine learning methods for mortality prediction in hospitalized patients—model establishment, internal and external validation, and visualization. *Journal of Translational Medicine*, 23(1), 97.
- [20] Lin, T. H., Chung, H. Y., Jian, M. J., Chang, C. K., Lin, H. H., Yen, C. T., ... & Shang, H. S. (2025). AI-Driven Innovations for Early Sepsis Detection by Combining Predictive Accuracy With Blood Count Analysis in an Emergency Setting: Retrospective Study. *Journal of Medical Internet Research*, 27, e56155.
- [21] Sater, M. S., Almansour, N., Malalla, Z. H., Ali, M. E., Fredericks, S., & Giha, H. A. (2025). Serum platelets and bilirubin levels as potential predictors of septic shock in adults with sepsis admitted to the intensive care unit. *Int. J. Clin. Exp. Med.*
- [22] Chen, S., Fan, J., Alaei, K., Placencia, G., Pishgar, E., & Pishgar, M. (2025). XGBoost-Based Prediction of ICU Mortality in Sepsis-Associated Acute Kidney Injury Patients Using MIMIC-IV Database with Validation from eICU Database. *medRxiv*, 2025-02.
- [23] Roccaforte, V., Sabbatini, G., Panella, R., Daves, M., Formenti, P., Gotti, M., ... & Pastori, S. (2025). The potential role of leukocytes cell population data (CPD) for diagnosing sepsis in adult patients admitted to the intensive care unit. *Clinical Chemistry and Laboratory Medicine (CCLM)*, (0).
- [24] Apalak, M., & Kiasaleh, K. (2024). Advancing early detection of Sepsis with temporal Convolutional Networks using ECG signals. *IEEE Access*, 12, 3417-3427.
- [25] A. E. W. Johnson, T. J. Pollard, L. Shen, L.-W.-H. Lehman, M. Feng, M. Ghassemi, B. Moody, P. Szolovits, L. A. Celi, and R. G. Mark, “MIMIC-III, a freely accessible critical care database,” *Sci. Data*, vol. 3, no. 1, pp. 1–9, May 2016.
- [26] Appadurai, J. P., Rajesh, T., Yugha, R., Sarkar, R., Thirumalraj, A., Kavim, B. P., & Seng, G. H. (2024). Prediction of EV charging behavior using BOA-based deep residual attention network. *Revista Internacional de Metodos Numericos para Calculo y Diseno en Ingenieria*, 40(2), 16.
- [27] C. W. Seymour, V. X. Liu, T. J. Iwashyna, F. M. Brunkhorst, T. D. Rea, A. Scherag, and G. Rubinfeld, “Assessment of clinical criteria for sepsis: For the third international consensus definitions for sepsis and septic shock (sepsis-3),” *J. Amer. Med. Assoc.*, vol. 315, no. 8, pp. 762–774, 2016.
- [28] Yang, Y., Chen, H., Heidari, A. A., & Gandomi, A. H. (2021). Hunger games search: Visions, conception, implementation, deep analysis, perspectives, and towards performance shifts. *Expert Systems with Applications*, 177, 114864.
- [29] Uma Maheswari, V., Stephe, S., Aluvalu, R., Thirumalraj, A., & Mohanty, S. N. (2024). Chaotic satin bowerbird optimizer based advanced AI techniques for detection of COVID-19 diseases from CT scans images. *New Generation Computing*, 42(5), 1065-1087.
- [30] Gunapriya, B., Thirumalraj, A., Anusuya, V. S., Kavim, B. P., & Seng, G. H. (2024). A Smart Innovative Pre-Trained Model-Based QDM for Weed Detection in Soybean Fields. In *Advanced Intelligence Systems and Innovation in Entrepreneurship* (pp. 262-285). IGI Global.
- [31] S.Jenifer, M J, Carmel Mary Belinda. (2023). Convolutional Neural Networks for Medical Image Segmentation and Classification: A Review. *Journal of Information Systems and Telecommunication (JIST)*, 44(11), 347-358.